Physics Letters B 741 (2015) 128–133

Contents lists available at ScienceDirect

Physics Letters B

www.elsevier.com/locate/physletb

Separation of the $1^+/1^-$ parity doublet in ^{20}Ne

J. Beller [a], C. Stumpf [a], M. Scheck [a,b,c], N. Pietralla [a,*], D. Deleanu [e], D.M. Filipescu [e], T. Glodariu [e], W. Haxton [f], A. Idini [a], J.H. Kelley [h], E. Kwan [d,1], G. Martinez-Pinedo [a,g], R. Raut [d,2], C. Romig [a], R. Roth [a], G. Rusev [d,3], D. Savran [i,j], A.P. Tonchev [d,4], W. Tornow [d], J. Wagner [a], H.R. Weller [d], N.-V. Zamfir [e], M. Zweidinger [a]

[a] Institut für Kernphysik, TU Darmstadt, D-64289 Darmstadt, Germany
[b] School of Engineering, University of the West of Scotland, Paisley PA1 2BE, UK
[c] SUPA, Scottish Universities Physics Alliance, Glasgow G12 8QQ, UK
[d] Triangle Universities Nuclear Laboratory, Duke University, Durham, NC, USA
[e] Horia Hulubei National Institute of Physics and Nuclear Engineering, ELI-NP, Bucharest-Magurele, Romania
[f] University of California, Berkeley, CA, USA
[g] GSI Helmholtzzentrum für Schwerionenforschung, D-64291 Darmstadt, Germany
[h] Triangle Universities Nuclear Laboratory, North Carolina State University, Raleigh, NC, USA
[i] ExtreMe Matter Institue EMMI and Research Division, GSI Helmholtzzentrum für Schwerionenforschung, D-64291 Darmstadt, Germany
[j] Frankfurt Institute for Advanced Studies FIAS, D-60438 Frankfurt am Main, Germany

ARTICLE INFO

Article history:
Received 30 July 2014
Received in revised form 5 December 2014
Accepted 6 December 2014
Available online 11 December 2014
Editor: D.F. Geesaman

Keywords:
Parity doublet
Parity violation

ABSTRACT

The $(J,T)=(1,1)$ parity doublet in ^{20}Ne at 11.26 MeV is a good candidate to study parity violation in nuclei. However, its energy splitting is known with insufficient accuracy for quantitative estimates of parity violating effects. To improve on this unsatisfactory situation, nuclear resonance fluorescence experiments using linearly and circularly polarized γ-ray beams were used to determine the energy difference of the parity doublet $\Delta E = E(1^-) - E(1^+) = -3.2(\pm 0.7)_{\mathrm{stat}}(^{+0.6}_{-1.2})_{\mathrm{sys}}$ keV and the ratio of their integrated cross sections $I^{(+)}_{s,0}/I^{(-)}_{s,0} = 29(\pm 3)_{\mathrm{stat}}(^{+14}_{-7})_{\mathrm{sys}}$. Shell-model calculations predict a parity-violating matrix element having a value in the range 0.46–0.83 eV for the parity doublet. The small energy difference of the parity doublet makes ^{20}Ne an excellent candidate to study parity violation in nuclear excitations.

1. Introduction

Since 1956, when Lee and Yang postulated a mirror-symmetry violation in β-decay [1] and 1957 when Wu experimentally verified the symmetry-violating effect [2], parity non-conservation is well established. These results are of paramount importance to our notion and understanding of fundamental symmetries in nature. While the strong force conserves parity, the effective nuclear force violates parity due to contributions of the weak interaction to the effective nucleon–nucleon interaction. Hence, various theoretical and experimental approaches have been employed to investigate parity violation in nuclei (Reviews in [3,4]). At the current stage, the weak meson–nucleon coupling constants deduced from various experiments are not consistent [5]. Further investigations of parity violation in nuclei are desirable.

In particular, studies of parity doublets $J^\pm$ are well suited to the observation of parity violation in nuclei. Depending on the details of the nuclear wave functions, the weak interaction matrix element between states of opposite parity is typically calculated to be on the order of 1 eV [3,5]. Due to the parity-violating character of the weak interaction, the physical $|\phi^\pm_J\rangle$ doublet states contain an admixture of the opposite parity, e.g.,

$$\left|\phi^-_J\right\rangle = \alpha\left|J^-\right\rangle + \beta\left|J^+\right\rangle, \tag{1}$$

with $\alpha^2+\beta^2=1$. Here, $|J^\pm\rangle$ denote the doublet eigenstates with good parity obtained from the parity-conserving part of the Hamiltonian. Within first-order perturbation theory, the contribution of

* Corresponding author.
E-mail address: beller@ikp.tu-darmstadt.de (J. Beller).

[1] Present address: National Superconducting Cyclotron Laboratory, Michigan State University, East Lansing, MI 48824, USA.
[2] Present address: UGC-DAE Consortium for Scientific Research, Kolkata Centre, Kolkata, India.
[3] Present address: Los Alamos National Laboratory, Los Alamos, NM, USA.
[4] Present address: Lawrence Livermore National Laboratory, Livermore, CA, USA.

http://dx.doi.org/10.1016/j.physletb.2014.12.018

the positive-parity eigenstate $|J^+\rangle$ to the physical state $|\phi_J^-\rangle$ is controlled by the matrix element of the parity non-conserving (PNC) interaction $V_{\rm PNC}$ and the energy splitting ΔE of the doublet states:

$$|\phi_J^-\rangle \approx |J^-\rangle + \frac{\langle J^+|V_{\rm PNC}|J^-\rangle}{\Delta E}|J^+\rangle, \tag{2}$$

and vice versa for the $|\phi_J^+\rangle$ state. Consequently, the opposite-parity admixture is enhanced if the energy splitting is small and the matrix element $\langle J^+|V_{\rm PNC}|J^-\rangle$ has a large value. Usually, contributions of the weak interaction to the nuclear effective Hamiltonian are not well known, comparatively small, and neglected.

In this respect, the $J^\pi = 1^+/1^-$ parity doublet in ^{20}Ne at 11.26 MeV excitation energy [6] has been suggested as one of the best cases for the study of parity violation in isolated nuclear eigenstates [7]. Their excitation energies are reported from different experiments [6] as 11.2623(19) MeV for the 1^+ state and 11.270(5) MeV for the 1^- state. Consequently, the energy difference of the doublet states is $\Delta E = E(1^-) - E(1^+) = 7.7 \pm 5.3$ keV, with a large relative uncertainty. Since the excitation energies were taken from different spectroscopic experiments, this difference may also be subject to additional systematic errors.

Recently, scattering of circularly polarized photons on strongly excited parity doublets has been proposed [7] as a promising tool for such studies. Despite the fact that the magnitude of the effect due to parity violation is small, on the order of 10^{-7}, dynamical and kinematical nuclear enhancements are expected to allow for its observation. However, as the large error demonstrates, the effective nuclear enhancement factor $\mathfrak{F}_e = |R_N/\Delta E| = (670 \pm 700)$ MeV^{-1} is not known to a sufficient precision[5] to make quantitative proposals for such investigations possible. Here, ΔE denotes the energy splitting of the parity doublet and $R_N = \sqrt{\Gamma_0(1^+)/\Gamma_0(1^-)}$ is the ratio of ground-state decay widths of unnatural to natural parity states. The major contribution to the large uncertainty of the nuclear enhancement factor is due to the energy difference of the parity doublet, which is measured with low accuracy: $\Delta E = 7.7 \pm 5.3$ keV [6]. Other contributions to the uncertainty of $\mathfrak{F}_e$ stem from the ground-state decay widths $\Gamma_0(1^\pm)$. Previously, the excitation energies $E(1^\pm)$ and $\Gamma_0(1^\pm)$ of the $1^+/1^-$ states were measured independently using different reactions. The 1^+ state has a significantly larger ground-state decay width $\Gamma_0(1^+)$ as compared to $\Gamma_0(1^-)$ for the near-by 1^- state. Therefore, the 1^+ state was observed in (e, e') [8] and (γ, γ') [9] experiments. The 1^- state, however, was observed in ^{16}O(α, γ) experiments [10–12].

The aim of this work is to establish the energy splitting ΔE of the $1^+/1^-$ parity doublet of ^{20}Ne and to simultaneously determine the ratio of decay matrix elements R_N from a single dedicated experiment which is designed to be sufficiently sensitive to both states. To this end, a unique combination of Nuclear Resonance Fluorescence (NRF) measurements using circularly and linearly polarized γ-ray beams was employed. Photon beams are maximally sensitive to nuclear dipole excitations. Its different polarization states allow to uniquely discriminate the parity of the nuclear wave functions with a close-to-ideal polarization sensitivity of ∼90%.

The experimental setup is outlined in Section 2 and the data analysis in Section 3. In Section 4, shell-model calculations to estimate the parity-violating transition matrix element in Eq. (2) are presented making use of two different effective interactions [13,14] and the parity-violating Desplanques, Donoghue, Holstein potential [3,5]. In Section 5 experimental requirements for the measurement of the parity violation are discussed.

2. Experiment

Linearly and circularly polarized γ-ray beams of energy $E_\gamma = 11.26(35)$ MeV were provided by the HIγS facility at Triangle Universities Nuclear Laboratory in Durham, NC, USA [15]. Electron bunches injected into the Duke storage ring pass a wiggler system of the Duke free electron laser (FEL) and emit FEL photons. Depending on the orientation of the wiggler magnets (linear or helical) the FEL photons can be either linearly or circularly polarized. The FEL photons are reflected by a mirror and Compton-backscattered from subsequent electron bunches. Compton back-scattering at a scattering angle of $\theta = 180°$ conserves the polarization of the photons and boosts the eV photon energies to the MeV range. Variation of the electron energy and the wiggler magnet current makes it possible to tune the γ-ray energy to the required energy of 11.26 MeV.

The detector setup was placed 60 m downstream of the collision point. A lead collimator limited the Compton back-scattered γ-ray beam to a small angular range and, therefore, to a narrow spectral distribution ($\Delta E \approx 3\%$).

The target nuclei were excited by resonant absorption of photons. The target consisted of natural Ne gas (90.48% ^{20}Ne) pressurized to 170 bar. The gas was stored in a container [16] consisting of an aluminum core wrapped in carbon fiber which was orientated along the beam axis. Its effective length was 11.4 cm resulting in an effective target thickness of 1.73 g/cm^2. The target holder was a 5 cm thick Pb ring which also shielded the downstream end of the container including the filling valve made of brass. A ^{28}Si target was attached to the upstream end of the target container for use in a simultaneous energy-calibration measurement. The de-exciting γ-ray transitions at energies

$$E_\gamma = E_x\left(1 - \frac{E_x}{2Mc^2}\right) \tag{3}$$

were studied with four high-purity germanium (HPGe) detectors surrounding the target at a polar angle $\vartheta = 90°$ relative to the beam axis, where E_x is the intrinsic excitation energy and the second term on the RHS of Eq. (3) represents the recoil correction. Two detectors were positioned parallel and two perpendicular to the horizontal polarization plane. Each of the detectors has an efficiency of 60% relative to a $3'' \times 3''$ standard NaI detector.

The angular distribution function for a $0^+ \xrightarrow{\vec{\gamma}} 1^\pm \xrightarrow{\gamma} 0^+$ NRF cascade using 100% linearly polarized γ-rays, as it occurs in the case of ^{20}Ne, is given by [17–19]

$$W(\vartheta, \varphi) = 1 + \frac{1}{2}\left[P_2(\cos\vartheta) + \frac{1}{2}\pi\cos(2\varphi)P_2^{(2)}(\cos\vartheta)\right], \tag{4}$$

where π denotes the parity of the excited $J = 1$ state, and ϑ and φ denote the polar and azimuthal angle, respectively. The terms $P_2(\cos\vartheta)$ and $P_2^{(2)}(\cos\vartheta)$ denote the second order ordinary and unnormalized associated Legendre polynomials. The angular distribution for excitation using circularly polarized γ-rays is given as

$$W_\circ(\vartheta) = 1 + \frac{1}{2}P_2(\cos\vartheta). \tag{5}$$

The angular distribution functions for $E1$ ($\pi = -$) and $M1$ ($\pi = +$) transitions as given by Eq. (4) along with a schematic plot of the detector arrangement are shown in Fig. 1. Photons emitted in the $0^+ \xrightarrow{\vec{\gamma}} 1^+ \xrightarrow{\gamma} 0^+$ cascade are preferentially detected within the polarization plane defined by the electric field vector of the γ-ray

[5] The uncertainty was given erroneously in Ref. [7] as 7000 MeV^{-1}.

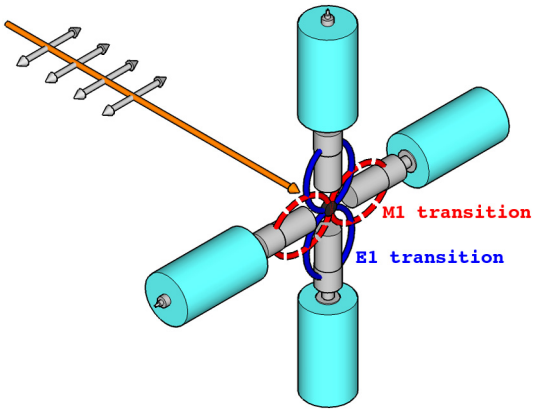

Fig. 1. (Color online.) Schematic view of the NRF setup. The incoming beam is horizontally polarized and hits the target in the middle of the detector setup. The dashed red curve shows the emission in case of an $M1$ transition and the solid blue curve illustrates the emission in case of an $E1$ transition.

beam. The decay photons of a $0^+ \xrightarrow{\vec{\gamma}} 1^- \xrightarrow{\gamma} 0^+$ cascade are preferentially emitted in the direction perpendicular to the polarization plane. Thus, by measuring the NRF intensities in both planes it is possible to separate $J^\pi = 1^\pm$ states with respect to their parity.

Since the states of the parity doublet have different parities, they can be separated by this method. Due to the finite target and detector sizes, the separation will, of course, not be complete. Indeed, the polarization sensitivity

$$q = \frac{|I_\gamma^\parallel - I_\gamma^\perp|}{I_\gamma^\parallel + I_\gamma^\perp} \tag{6}$$

of the setup has been reported to be 0.9 in previous experiments (e.g., see [20]). Here, $I_\gamma^\parallel$ ($I_\gamma^\perp$) denote the actual experimental yields in the (finite) detectors for a $0^+ \to 1^\pm \to 0^+$ cascade parallel (perpendicular) to the polarization plane. Thus, the γ-ray intensity of the $0^+ \to 1^+ \to 0^+$ ($0^+ \to 1^- \to 0^+$) cascade will be suppressed by a factor $(1-q)/(1+q) \approx 1/20$ in the vertical (horizontal) spectrum. Therefore, even though the $0^+ \to 1^+ \to 0^+$ cascade is expected to be about 44 times stronger [6], an identification of the $0^+ \to 1^- \to 0^+$ cascade is possible in the vertical spectrum.

Two measurements were performed on ^{20}Ne at a γ-ray beam energy of 11.26 MeV and a spectral width of 3%. In one measurement a linearly polarized photon beam was used to separate the parity doublet. A second measurement with circularly polarized photon beams was performed to obtain a consistent energy and efficiency calibration for all detectors. Here, the angular distributions of the scattered γ rays have no azimuthal dependence and the deexciting transitions of the parity doublet and of the excited states in the calibration target have the same intensities in every detector. The obtained spectra are shown in Fig. 2. The HPGe detectors have an energy resolution of 7.5 keV at 11.4 MeV. The simultaneously irradiated ^{28}Si target has a 1^+ state at 11.45 MeV [21], which is exploited to extract the polarization sensitivity of the setup and the peak shapes of the individual detectors. In addition, the 1^+ state of ^{28}Si at 11.45 MeV together with its single-escape peak deliver a consistent energy calibration for each detector.

3. Analysis

The parity-doublet states are too close in energy to resolve them individually within the detector resolution of 7.5 keV. Therefore, only summed peaks are observed. However, the positions and peak areas of the centroids of the parity doublet change when switching from circularly to linearly polarized photon beams because of their dependence on the azimuthal observation angles with respect to the polarization plane of the incident γ-ray beam. Consequently, the intensities of the $1^\pi \to 0_1^+ E1$ or $M1$ transition will be enhanced or suppressed in a different way. The circularly polarized γ-ray beam cannot induce any azimuthal anisotropy and is perfectly suited for the production of an azimuthal calibration point. The analysis was performed assuming that the γ-ray beam was 100% circularly polarized. Small deviations would deliver additional systematic uncertainties which are not considered here. The observed energy centroid for linear polarization in the polarization plane is given by

$$E_\parallel = \frac{E_\gamma(1^-) I_{s,0}^{(-)}(1-q) + E_\gamma(1^+) I_{s,0}^{(+)}(1+q)}{I_{s,0}^{(-)}(1-q) + I_{s,0}^{(+)}(1+q)}, \tag{7}$$

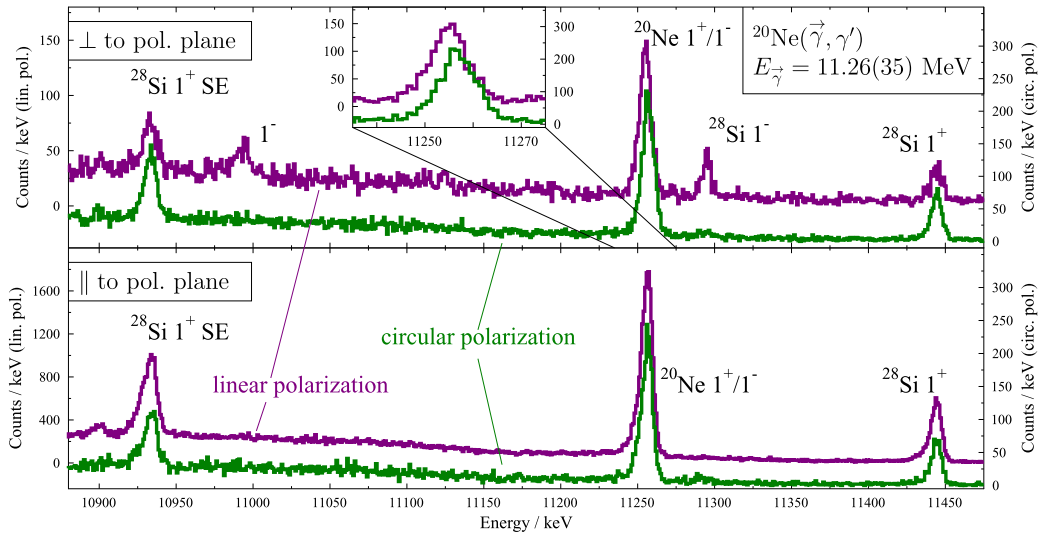

Fig. 2. (Color online.) The summed spectra for the detectors positioned vertical (top) and horizontal (bottom) to the polarization plane. For a better comparison between spectra obtained either with linear polarization or with circular polarization two different scales are used to account for varying count rates and data acquisition time periods. The spectra obtained with an incoming linearly polarized beam (purple) use the left axis, while the spectra obtained with an incoming circularly polarized beam (green) use the right axis. The energy difference between the ^{20}Ne doublet states is determined from the small energy shift between linear and circular polarization in the vertical detectors which is enlarged in the inlay.

Table 1
Measured γ-ray centroids and peak areas for the $1^{\pm}$ parity doublet of ^{20}Ne at 11.26 MeV for different azimuthal angles and beam polarizations.

Beam pol.	Observable	Horizontal	Vertical
Circular	$E_\circ$ [keV]	11 255.2(2)	11 255.1(2)
Circular	Area $A_\circ$	2014(51)	2139(53)
Linear	$E_{\parallel/\perp}$ [keV]	11 255.2(1)	11 253.6(2)
Linear	Area $A_{\parallel/\perp}$	16 272(150)	1291(46)

Table 2
Results and comparison to literature for the deduced level energies of the 1^+ and 1^- states, their energy splitting ΔE, their ratio of integrated cross sections, and their nuclear enhancement factor $\mathfrak{F}_e$.

Observable	This work	Ref. [6]
$E(1^+)$ [keV]	11 258.6(2)[a]	11 262.3(19)
$E(1^-)$ [keV]	$11\,255.4(\pm0.7)_{\rm stat}(^{+1.2}_{-0.6})_{\rm sys}$	11270(5)
ΔE [keV]	$-3.2(\pm0.7)_{\rm stat}(^{+0.6}_{-1.2})_{\rm sys}$	7.7 ± 5.5
$I^{(+)}_{s,0}/I^{(-)}_{s,0}$	$29(\pm3)_{\rm stat}(^{+14}_{-7})_{\rm sys}$	44 ± 13
$\mathfrak{F}_e$ [keV^{-1}]	$1.4(\pm0.3)_{\rm stat}(\pm0.2)_{\rm sys}$[b]	0.67 ± 0.70[c]

[a] Relative to 1^+ state of ^{28}Si.
[b] Correcting for the known decay ratios Γ_0/Γ [6].
[c] Taken from Ref. [7] in which the uncertainty was erroneously given as 7 keV^{-1}.

and when perpendicular to the polarization plane, it is given by

$$E_\perp = \frac{E_\gamma(1^-)I^{(-)}_{s,0}(1+q) + E_\gamma(1^+)I^{(+)}_{s,0}(1-q)}{I^{(-)}_{s,0}(1+q) + I^{(+)}_{s,0}(1-q)}. \tag{8}$$

The case of circularly polarized beam is given by

$$E_\circ = \frac{E_\gamma(1^-)I^{(-)}_{s,0} + E_\gamma(1^+)I^{(+)}_{s,0}}{I^{(-)}_{s,0} + I^{(+)}_{s,0}}, \tag{9}$$

where $I^{(+,-)}_{s,0}$ indicate elastic photon-scattering cross sections of the 1^+ and 1^- states, respectively. $A_\parallel$ and $A_\perp$ are the peak area of the parity doublet in the parallel and horizontal detectors obtained using the linearly polarized γ-ray beam. Their ratio amounts to

$$\frac{A_\parallel}{A_\perp} = \frac{\epsilon_\parallel}{\epsilon_\perp}\frac{(1-q)I^{(-)}_{s,0} + (1+q)I^{(+)}_{s,0}}{(1+q)I^{(-)}_{s,0} + (1-q)I^{(+)}_{s,0}}. \tag{10}$$

The relative detector efficiency is directly proportional to the relative peak areas observed with circularly polarized γ-ray beam $\epsilon_\parallel/\epsilon_\perp \propto A^\parallel_\circ/A^\perp_\circ$ and amounts to 0.956(34) taking the different detector live times into account. The polarization sensitivity of our setup was derived from a geometrical analysis to $q = 0.92(2)$. The effective angular distribution due to the extended target was integrated over the detector opening angles. The associated uncertainties generate a systematical error in the determination of the energy splitting and of the ratio of the integrated cross sections of the parity doublet.

The primary observables of our measurement are four peak centroids and their respective peak areas for the cases of linear and circular polarized beams with observations in both the horizontal and vertical directions. They are given in Table 1. These observables enable us to determine the recoil-corrected excitation energies of the parity doublet $E(1^\pm)$, their difference ΔE, the ratio of the integrated cross sections $I^{(+)}_{s,0}/I^{(-)}_{s,0}$, and the nuclear enhancement factor $\mathfrak{F}_e$. These values are given in Table 2.

The newly derived ratio $I^{(+)}_{s,0}/I^{(-)}_{s,0}$ is in fair agreement with previous data obtained from separate measurements (see Table 2). With this we obtain from Eqs. (7)–(9) the energy difference of the doublet states as

$$\begin{aligned}\Delta E &= E(1^-) - E(1^+)\\ &= \left(1 + \frac{1-q}{1+q}\frac{I^+}{I^-}\right)(E_\perp - E_\parallel)\\ &= -3.2(\pm0.7)_{\rm stat}(^{+0.6}_{-1.2})_{\rm sys}\ \text{keV}.\end{aligned} \tag{11}$$

This value is more precise than previous literature. It was obtained from a single measurement and suffers less from systematical errors. In addition, it can clearly be inferred that the energetic ordering of those two states was incorrectly given in the literature. The 1^- state is lower in energy by about 3 keV than the 1^+ state. This level ordering is evident in the spectra (compare Fig. 2 and Table 1). The doublet peak observed perpendicularly to the polarization plane is shifted to lower energies when switching from circular to linear polarization. Since the signal from the 1^- state is enhanced at this observation angle in the measurement with linearly polarized γ-ray beam as compared to circularly polarized γ-ray beam, the 1^- state must be located below the 1^+ state. This observation is owed to the fact that in the present measurement both states were excited simultaneously and, therefore, a high-precision relative measurement could be performed. Finally, we obtain a more precise value for the nuclear enhancement factor $\mathfrak{F}_e$.

4. Theory

We estimate the parity-violating matrix element $\langle J^+|V_{\rm PNC}|J^-\rangle$ using the valence-space shell model. These shell-model calculations are challenging since it is necessary to describe both positive- and negative-parity states in the same valence space. We employ two different interactions, the traditional ZBM interaction [13] and the more recent PSDPF interaction [14]. This allows us to check the robustness of the matrix element with respect to different choices of the valence space. The ZBM interaction uses a ^{12}C core and a valence space comprising the $1p_{1/2}$, $1d_{5/2}$ and $2s_{1/2}$ orbitals. This interaction was adjusted to reproduce the structure of nuclei around ^{16}O including the coexistence between spherical and deformed states. Since the ZBM interaction does not allow for excitations from the $1p_{3/2}$ orbit to the *sd* shell, we probe the effect of these excitations on the matrix element by comparing to results obtained using the PSDPF interaction. This interaction is based on a ^{4}He core and includes the full *p*, *sd* and *pf* shells into the valence space. It provides a good reproduction of the observed coexistence in *sd*-shell nuclei between natural parity states, assumed to be $0\hbar\omega$, and intruder states, assumed to be $1\hbar\omega$. The eigenstates have been computed with our newly developed shell-model code [22], which is capable of calculating matrix elements of two- and many-body operators. We have benchmarked all shell-model calculations versus the Antoine code [23–25]. When using the PSDPF valence space, we have investigated the impact of possible center-of-mass contaminations by including a Lawson-type center-of-mass Hamiltonian $\lambda H_{\rm cm}$ with $\lambda = 1$ and 10 for the solution of the eigenvalue problem. The effect of center-of-mass contaminations on the energies and the matrix element is negligible. We obtain a deviation of less than 0.5% for the matrix element for the two choices of λ.

In the shell-model calculation using the ZBM interaction, we obtain the 1^+ and 1^- states at an excitation energy of 10.966 MeV and 10.457 MeV, respectively, with an energy splitting of 509 keV. For the PSDPF interaction, the corresponding excitation energies are 11.196 MeV and 11.428 MeV and the energy difference is 226 keV. For the two interactions considered here, the positive- and negative-parity eigenstates, respectively, have similar structure. For the positive-parity eigenstate, the leading configurations including the core orbits are $(1s_{1/2})^2(1p_{3/2})^4(1p_{1/2})^2(1d_{5/2})^2$

Table 3
Individual components of the parity-violating matrix element of the $1^+/1^-$ parity doublet of ^{20}Ne computed in the shell model using the ZBM [13] and PSDPF [14] interaction. The second column gives the "best values" for the coupling constants as proposed by Desplanques et al. [26]. The matrix elements for the different components of the DDH interaction have been computed including and neglecting short-range correlations. See text for additional information.

Component	Coupling (10^{-6})	m.e. ZBM		m.e. PSDPF	
		Without SRC	With SRC	Without SRC	With SRC
F_0	1.59	0.438 MeV	0.128 MeV	0.672 MeV	0.230 MeV
F_2	1.33	0.019 MeV	0.006 MeV	0.020 MeV	0.010 MeV
G_0	0.80	0.114 MeV	0.028 MeV	0.160 MeV	0.045 MeV
Total		0.81 eV	0.23 eV	1.22 eV	0.42 eV
Constraint from Ref. [5]		1.48 eV	0.46 eV	2.42 eV	0.83 eV

$(2s_{1/2})^0$ and $(1s_{1/2})^2(1p_{3/2})^4(1p_{1/2})^2(1d_{5/2})^1(2s_{1/2})^1$ for both protons and neutrons. The configurations contributing to the negative-parity eigenstate are more evenly distributed. The main contribution consists of one particle–hole excitation on top of the positive parity wave function, with one particle excited from the $1p_{1/2}$ orbit to the $1d_{5/2}$ or $2s_{1/2}$ orbit. We do not observe significant differences in the eigenstates for the different valence spaces and interactions. Using these eigenstates, we calculate the matrix element of the parity-violating Desplanques, Donoghue, Holstein (DDH) potential [26,3] which arises from single- and multi-pion and vector meson exchanges. The potential contains several isoscalar, isovector and isotensor components, each associated with a coupling constant. As the 1^+ and 1^- states of ^{20}Ne have isospin $T = 1$ and $T_z = 0$, only the isoscalar and isotensor components contribute. The relevant DDH "best values" [26] of the coupling constants are given in Table 3. We use the same numerical two-body matrix elements as done in Ref. [3] and have cross-checked our implementation against results for ^{18}F and ^{19}F reported there.

Short-range correlations can be potentially important for the isoscalar and isotensor components of the matrix element. They correspond to ρ- and ω-meson exchanges in the DDH potential, and thus involve momentum scales significantly above those included in the shell model wave functions. We have evaluated the effects of short-range correlations (SRC) using the function of Miller and Spencer [27] We found that it suppresses the matrix elements by a factor of 3 (see Table 3). An additional source of uncertainty is related to the value of the coupling constants. A recent analysis by Haxton and Holstein [5] of the available PNC data – including the asymmetries at various energies for $p + p$, the $p+^4$He asymmetry, and results from ^{18}F and ^{19}F – indicate that the isoscalar couplings that dominate the matrix elements of interest fulfill the following constraint

$$F_0 + 0.23G_0 = (3.6 \pm 0.8) \times 10^{-6}. \tag{12}$$

Neglecting the small contribution of the isotensor component F_2, the parity violating matrix element of ^{20}Ne can be written as:

$$\begin{aligned}\langle 1^+|V_{\mathrm{PNC}}|1^-\rangle &= F_0\langle V^{F_0}\rangle + G_0\langle V^{G_0}\rangle \\ &= \left[F_0 + \frac{\langle V^{G_0}\rangle}{\langle V^{F_0}\rangle}G_0\right]\langle V^{F_0}\rangle \\ &\approx (F_0 + 0.23\,G_0)\langle V^{F_0}\rangle,\end{aligned} \tag{13}$$

where in the last expression the factor 0.23 represents an average of the ratio of matrix elements obtained by the ZBM and PSDPF interactions that is almost not sensitive to the inclusion of a SRC. The numbers shown in the last row of Table 3 have been evaluated using Eq. (13). We conclude that the current "best estimate" for the ^{20}Ne matrix element is ∼0.46–0.83 eV, based on the ZBM and PSDPF results of Table 3. The individual contributions and the total matrix element are of the same order of magnitude as the other parity doublets considered in Ref. [3]. In particular the ^{18}F, ^{19}F, and ^{20}Ne doublets are very similar in their PNC mixing strengths. Similar to the other doublets discussed in Ref. [3], we observe a slight increase in the PSDPF matrix element compared to that for the ZBM interaction. The former includes a very limited set of multi-$\hbar\omega$ excitations, but employs a larger single-particle space that is separable, which allows us to project center-of-mass motion exactly. Based on treatments of ^{18}F and ^{19}F that used even larger separable spaces of the PSDPF type that included all $2\hbar\omega$ configurations, one might expect a substantial reduction in the PSDPF matrix elements when such configurations are included. In fact, we have done a preliminary calculation of this type, using an interaction that very successfully reproduced the spectrum of ^{16}O in a full $(0 + 2 + 4)\hbar\omega$ calculation [28]. (This interaction differs in some important respects from those that were used in earlier ^{18}F and ^{19}F calculations [3].) We do find some reduction in the matrix elements when the positive-parity shell-model space is increased from $0\hbar\omega$ to $(0 + 2)\hbar\omega$, but the reduction is modest compared to the reductions found in ^{18}F and ^{19}F, a factor of ∼0.87. While further study of both the ^{20}Ne matrix element and its relationship to those in ^{18}F and ^{19}F is needed, our present conclusion is that the matrix element is likely in the range of 0.46–0.83 eV.

5. Discussion

The observation of parity-violating effects in nuclei is an experimental challenge. Based on the measured splitting of the parity-doublet states of ^{20}Ne and the calculated parity-violating matrix element, we expect a parity admixture β according to Eqs. (1) and (2) of the order of 10^{-4}.

One possibility to measure such a small admixture is to excite exclusively the 1^- state using a 100% linearly polarized γ-ray beam with a sufficiently small bandwidth i.e., about a hundred times better than what is available today. Using an HIγS-like setup one could measure the $M1$ admixture of the de-excitation process

$$\begin{aligned}&\langle 0^+|T(M1) + T(E1)|\phi_1^-\rangle \\ &\quad = \alpha\langle 0^+|T(E1)|1^-\rangle + \beta\langle 0^+|T(M1)|1^+\rangle.\end{aligned} \tag{14}$$

However, the $E1$ ($M1$) NRF photons are emitted preferably perpendicular (parallel) to the polarization plane, see Eq. (4). Therefore, it would be possible to disentangle the $E1$ and $M1$ contribution of the ground-state decay of the 1^- state using known angular distributions. Placing detectors perpendicular and parallel to the polarization plane at $\vartheta = 90°$ relative to the incoming beam, numbers of events

$$N^{\perp} = N_T N_\gamma \epsilon\left((1+q)\alpha^2 I_{s,0}^{(-)} + \underbrace{(1-q)\beta^2}_{\approx 0} I_{s,0}^{(+)}\right) \tag{15}$$

and

$$N^{\parallel} = N_T N_\gamma \epsilon\left((1-q)\alpha^2 I_{s,0}^{(-)} + (1+q)\beta^2 I_{s,0}^{(+)}\right) \tag{16}$$

would be measured depending on the experimental polarization sensitivity q of the setup and, due to the opposite parity admixture, on β. Here, N_T denotes the number of target nuclei, N_γ the time-integrated γ-ray flux, and ϵ the detector efficiency. Combining Eqs. (15) and (16) yields

$$N^{\parallel} = \left(\frac{\beta^2}{\alpha^2}\frac{I_{s,0}^{(+)}}{I_{s,0}^{(-)}} + \frac{1-q}{1+q}\right)N^{\perp} = \left(\Re\langle PNC\rangle^2 + \frac{1-q}{1+q}\right)N^{\perp} \tag{17}$$

with the abbreviations

$$\Re \equiv \frac{I_{s,0}^{(+)}}{I_{s,0}^{(-)}}/\Delta E^2 = \frac{(\Gamma_0/\Gamma)_{1^-}}{(\Gamma_0/\Gamma)_{1^+}}\mathfrak{F}_e^2 \tag{18}$$

and

$$\langle PNC\rangle \equiv \left\langle J^+|V_{\mathrm{PNC}}|J^-\right\rangle = \beta\Delta E. \tag{19}$$

It allows to measure the parity-violating matrix element $\langle PNC\rangle$ directly.

By performing the same experiment on a different $J=1$ state which is not part of a parity doublet the polarization sensitivity q can be determined to a sufficient precision. This way, systematical errors such as the polarization sensitivity or detector efficiencies are reduced drastically.

The total number of events needed to achieve an observation of parity mixing of this doublet with a 99.95% confidence limit ("5σ-measurement") is given by

$$N^{\perp} \approx \frac{(1-q)/(1+q)}{4\Re^2\langle PNC\rangle^2\Delta\langle PNC\rangle^2}. \tag{20}$$

Using the values given in Table 2, $\Re$ amounts to $2.8(\pm1.2)_{\mathrm{stat}}(\pm0.9)_{\mathrm{sys}}$ keV^{-2}. However, we may safely assume that a facility which can deliver intense and monochromatic γ-ray beams one hundred times better than today could improve this value to an uncertainty of less than 2%. For an experimental sensitivity of $q=0.99$, a parity mixing of $\langle PNC\rangle = 1$ eV, and a required accuracy of $\Delta\langle PNC\rangle = 0.2$ eV a total of $N^{\perp} = 3\times10^9$ counts are required.

6. Conclusion

A combination of linearly and circularly polarized γ-ray beams enabled us to study the $1^+/1^-$ parity doublet of ^{20}Ne and to measure the energy splitting ΔE, the level ordering, and the ratio of integrated cross sections $I_{s,0}^{(+)}/I_{s,0}^{(-)}$, simultaneously. The energy splitting of about 3 keV combined with the shell-model estimate of parity violating matrix-element in the range 0.46–0.83 eV, make ^{20}Ne an intriguing candidate to study parity violation in nuclear excitations. The ^{20}Ne PNC doublet probes a combination of isoscalar couplings very similar to that tested in previous $p+p$ asymmetry measurements, but without the significant isotensor contribution that affects the $p+p$ asymmetry analysis. That contribution has typically been estimated using the DDH isotensor "reasonable range". But there is no guarantee that range is reasonable, as it is not constrained experimentally. In ^{20}Ne the isotensor contribution plays a much smaller role, a consequence of the averaging of the potential that comes with summing over core nucleons. Thus in principle, if ^{20}Ne nuclear structure uncertainties could be reduced, this doublet could provide a cleaner test of isoscalar PNC. This same argument is currently motivating lattice QCD studies of the isotensor meson–nucleon coupling.

Acknowledgements

We thank M. Fujiwara for discussions and the HIγS staff for providing excellent γ-ray beams. We thank F. Nowacki for providing us with the matrix-elements of the PSDPF interaction. This work was partly supported by the Deutsche Forschungsgemeinschaft under grant Contract No. SFB 634 and the Helmholtz Association through the Nuclear Astrophysics Virtual Institute (VH-VI-417). D. Deleanu, D.M. Filipescu, T. Glodariu, and N.V. Zamfir were supported by Extreme Light Infrastructure – Nuclear Physics (ELI-NP) – Phase I, a project co-financed by the Romanian Government and European Union through the European Regional Development Fund (425/12.12.2012, POS CCE, ID 1334 SMIS-CSNR 40741). D. Savran acknowledges support by the Alliance Program of the Helmholtz Association (HA216/EMMI).

References

[1] T.D. Lee, C.N. Yang, Phys. Rev. 104 (1956) 254.
[2] C.S. Wu, et al., Phys. Rev. 105 (1957) 1413.
[3] E.G. Adelberger, W.C. Haxton, Annu. Rev. Nucl. Sci. 35 (1985) 501.
[4] B. Desplanques, C.H. Hyun, S. Ando, C.-P. Liu, Phys. Rev. C 77 (2008) 064002.
[5] W.C. Haxton, B.R. Holstein, Prog. Part. Nucl. Phys. 71 (2013) 185.
[6] D.R. Tilley, et al., Nucl. Phys. A 636 (1998) 249.
[7] A.I. Titov, et al., J. Phys. G, Nucl. Part. Phys. 32 (2006) 1097.
[8] W.L. Bendel, et al., Phys. Rev. C 3 (1971) 1821.
[9] U.E.P. Berg, et al., Phys. Rev. C 27 (1983) 2891.
[10] D.J. Steck, Phys. Rev. C 17 (1978) 1034.
[11] J.M. Davidson, M.M. Lowry, Phys. Rev. C 18 (1978) 2776.
[12] L.K. Fifield, et al., Nucl. Phys. A 334 (1980) 109.
[13] A. Zuker, Phys. Rev. Lett. 23 (1969) 983.
[14] M. Bouhelal, et al., Nucl. Phys. A 864 (2011) 113.
[15] H.R. Weller, et al., Prog. Part. Nucl. Phys. 62 (2009) 257.
[16] T.C. Li, et al., Phys. Rev. C 73 (2006) 054306.
[17] N. Pietralla, H.R. Weller, V.N. Litvinenko, M.W. Ahmed, A.P. Tonchev, Nucl. Instrum. Methods A 483 (2002) 556.
[18] N. Pietralla, et al., Phys. Rev. Lett. 88 (2001) 012502.
[19] U. Kneissl, N. Pietralla, A. Zilges, J. Phys. G, Nucl. Part. Phys. 32 (2006) R217.
[20] J. Isaak, et al., Phys. Rev. C 83 (2011) 034304.
[21] P.M. Endt, Nucl. Phys. A 633 (1998) 1.
[22] R. Roth, et al., in preparation.
[23] E. Caurier, Shell model code ANTOINE, IRES, Strasbourg, 1989–2004.
[24] E. Caurier, F. Nowacki, Acta Phys. Pol. 30 (1999) 705.
[25] E. Caurier, et al., Rev. Mod. Phys. 77 (2005) 2.
[26] B. Desplanques, J.F. Donoghue, B.R. Holstein, Ann. Phys. (N.Y.) 124 (1980) 449.
[27] G.A. Miller, J.E. Spencer, Ann. Phys. 100 (1976) 562.
[28] W.C. Haxton, C. Johnson, Phys. Rev. Lett. 65 (1990) 1325.